# Correlation between the structural, morphological, optical, and electrical properties of $In_2O_3$ thin films obtained by an ultrasonic spray CVD process

A. Bouhdjer†, A. Attaf, H. Saidi, H. Bendjedidi, Y. Benkhetta, and I. Bouhaf

Laboratory of Semiconductors Materials, University of Med Kheider, BP 145 RP, 07000 Biskra, Algeria

**Abstract:** Indium oxide ($In_2O_3$) thin films are successfully deposited on glass substrate at different deposition times by an ultrasonic spray technique using Indium chloride as the precursor solution; the physical properties of these films are characterized by XRD, SEM, and UV–visible. XRD analysis showed that the films are polycrystalline in nature having a cubic crystal structure and symmetry space group Ia3 with a preferred grain orientation along the (222) plane when the deposition time changes from 4 to 10 min, but when the deposition time equals 13 min we found that the majority of grains preferred the (400) plane. The surface morphology of the $In_2O_3$ thin films revealed that the shape of grains changes with the change of the preferential growth orientation. The transmittance improvement of $In_2O_3$ films was closely related to the good crystalline quality of the films. The optical gap energy is found to increase from 3.46 to 3.79 eV with the increasing of deposition time from 4 to 13 min. The film thickness was varied between 395 and 725 nm. The film grown at 13 min is found to exhibit low resistivity ($10^{-2}$ Ω·cm), and relatively high transmittance (∼ 93%).

**Key words:** indium oxide; deposition time; ultrasonic spray; optical and electrical properties

**DOI:** 10.1088/1674-4926/36/8/082002 **EEACC:** 2520

## 1. Introduction

Transparent conductive oxide (TCO) thin films are technologically important due to their high optical transparency in the visible region, wide band gap and good electrical conductivity. Furthermore, among them, indium oxide ($In_2O_3$) thin film has received much attention. It is a wide band-gap semiconductor and has a band gap of 3.5–3.75 eV, a cubic (Ia3) structure of lattice constant 1.0117 nm, dielectric constant of 8.9, and refractive index 2.0–2.1[1]. It is frequently used for photovoltaic devices, transparent windows, liquid crystal displays (LCD), light emitting diodes (LED), solar cell, gas sensors and anti-reflecting coatings[2]. Many techniques have been successfully applied to deposited indium oxide thin films such as spray pyrolysis[3], vacuum evaporation[4], magnetron sputtering[5], DC-sputtering[6], sol gel[7], and pulsed laser ablation[8]. Among these, in this paper we will focus on the spray ultrasonic technique, which is a method suitable for large-scale production. It has several advantages in producing nanocrystalline thin films, such as, having a relatively homogeneous composition, it is inexpensive and permits easy deposition in the atmospheric condition. Due to the simple deposition on glass substrate because of the low substrate temperatures involved, it is possible to alter the mechanical, electrical, optical and magnetic properties of $In_2O_3$ nanostructures. The physical properties of undoped and doped $In_2O_3$ films obtained by the spray ultrasonic technique have been widely reported[9, 10], due to the greater interest of $In_2O_3$ thin films.

In this paper, $In_2O_3$ thin films were grown on glass substrate using the ultrasonic spray technique. The film's properties are dependent from the film deposition parameters such as the deposition time. We have studied the effect of the deposition time on the crystalline structure, morphologic, optical, and electrical properties of $In_2O_3$ thin films; and we evaluated the relationship between these properties in general.

## 2. Experimental procedure

Indium oxide was deposited by spraying an alcoholic solution containing a 0.1 M of indium chloride $InCl_3$ (Merk, 99.9), on glass substrates heated at 400 ℃. The glass substrates were kept in a detergent solution and cleaned with distilled water. Afterwards, the glass substrates were kept in a solution of methanol and cleaned for approximately 15 min. Finally, the glass plates were taken out of the ultrasonic bath and once again cleaned with distilled water. In all depositions the distance spray nozzle–substrate equals 4.5 cm. All the parameters were kept constant and only the film thickness was changed through the change of the deposition time. The structure and morphology of the films were analyzed by X-ray spectroscopy on a D8 ADVANCE Diffractometer using a Cu K$\alpha$ radiation ($\lambda$ = 1.5405 Å), JOEL model JSM 6301F scanning electron microscope, respectively, the optical transmittance spectra were obtained using a UV–VIS spectrophotometer. These measurements were performed using glass as the reference in a wavelength range of 200–800 nm. The electrical resistivity was determined using the four-point method.

## 3. Results and discussion

The XRD patterns for $In_2O_3$ thin films grown at various deposition times are shown in Figure 1. For the deposition time ($t$) equals 4 min the XRD spectrum of this sample exhibits a preferential orientation peak located at $2\theta = 30.69°$. However, we noticed the presence of a broad peak between 20° and 25°, indicating clearly the presence of an amorphous phase in

† Corresponding author. Email: adelbouhdjar@gmail.com
Received 27 January 2015, revised manuscript received 17 March 2015

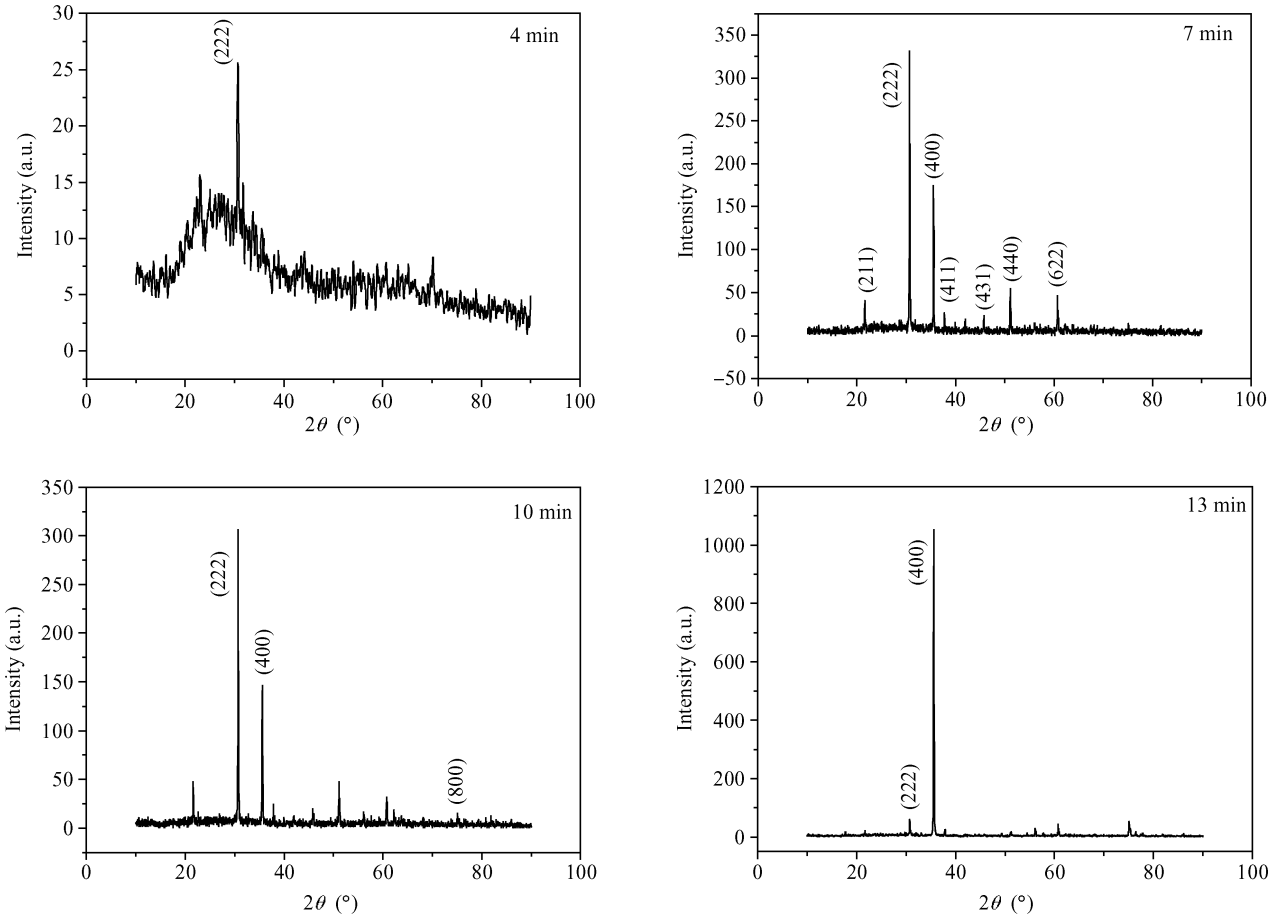


Figure 1. Evolution of the spectra of X-rays diffraction of $In_2O_3$ thin films for all deposition times.

the film network. This suggests that the structure of this film is heterogeneous, it is formed with small grains embedded in an amorphous phase in the film network. With increasing the deposition time by more than 4 min, we notice that the broad peak disappeared completely in addition to the presence of two main peaks and weak peaks: the two main peaks occur at $2\theta =$ 30.69° and 35.58°. These peaks correspond to the diffraction from the (222) and (400) planes of $In_2O_3$, respectively. The weak peaks centered at 21.77°, 37.80°, 45.69°, 51.23°, 60.69° and 75.01° are identified as $In_2O_3$ (211), (411), (431), (440) (622) and (800) planes, respectively. All peaks from XRD patterns coincide well with those given in the JCPDS data card (6-416)[11]. The $In_2O_3$ thin films are polycrystalline and crystallize in a cubic structure. The preferred growth orientation of $In_2O_3$ thin films depends on the deposition time. The intensity ratio of the (400) to (222) reflection is used to evaluate the deposition time effect on the film texture of the films, as shown in Figure 2. Depending on the results of the current study we found that the ratio I(400)/I(222) increases with the increasing of deposition time from 4 to 7 min. Then it decreases slightly as the deposition time was 10 min. Finally it increases considerably for 13 min and the (400) orientation becomes predominant. Korotcenkov *et al.* presented that the ratio I(400)/I(222) increased with the increase of spray pyrolysis temperature in sprayed $In_2O_3$[12] or the increase of film thickness[13]. They have also found that the peak intensity ratio of I(400)/I(222) increases with increasing film thickness[14]. The I(400)/I(222) ratio suggests that films deposited at 4, 7 and 10 min possess a strong crystallographic texture along the [111] direction and when the deposition time increased to 13 min, the texture is changed to the [100] direction. The preferential orientation development of crystalline grains mainly depends on the initial orientations during the nucleation process. For the deposition time equals 4 min, the (222) nucleation is a primary nucleation due to the surface free energy of the formation of the main planes of the $In_2O_3$ bixbyite phase, the (111) texture is expected since the high atomic density (111) plane of the bixbyite presents a lower surface free energy plane, as it has been previously discussed[15], and this accounts for the presence of one diffraction peak for $t = 4$ min. However, with increasing of deposition time more than 4 min, the growth of nuclei takes place due to the surface diffusion of the impinging solution sprayed. Then the (400) nucleation can be formed competitively with the (222) nucleation. In the same regard, Lee *et al.* found that the nuclei number increases with the increase of deposition time, and it will grow as well[16]. Finally the (400) nucleation is preferred for 13 min, and a strict improvement in preferred growth is observed. This can be explained as follows: with the increasing of deposition time the thickness of the film increases ($d =$ 725 nm for $t = 13$ min), which will prevent the incorporation of oxygen in the structure[17], leading to the preferred growth of (400)-grains. Several studies revealed that if the film contains sufficient oxygen, the crystal growth is preferentially with (222)-oriented grains, otherwise, the crystal growth is much

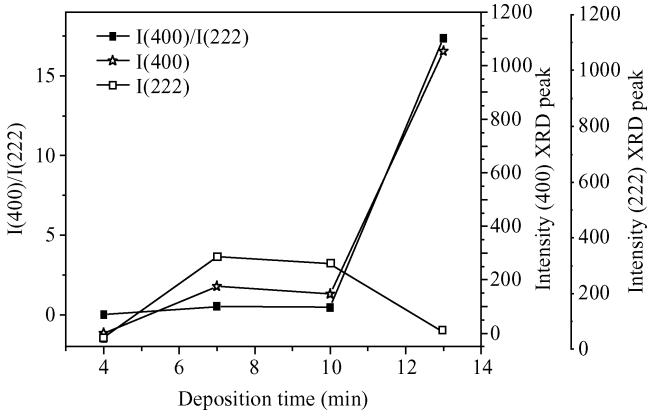


Figure 2. Deposition time effect on the film texture.

faster, with (400) orientation[18–20]. On the other hand, it was mentioned that the growth of the (222)-grains is suppressed with increasing thickness[21]. This goes in harmony with the XRD analysis, which indicates that with the deposition time increasing, the intensity of the plane (222) decreases (see Figure 2). In addition, the promotion of (400) plane texturing has also been associated with improvement in crystallinity in these cases. A similar effect has been observed by Saxena *et al.*[22] in their study of thickness dependence on the structural properties of films prepared by spray pyrolysis. On the other hand, the change in the strongest orientation of the XRD peak is correlated with the change in grain shapes as observed by SEM analysis (explained later). This probably indicates that the deposition time influences the evolution of microstructures and thereby reflects on the strongest orientation observed by XRD studies.

The average grain size $D$ of $In_2O_3$ is estimated using Scherrer's formula[23]:

$$D = \frac{0.9\lambda}{\beta \cos\theta}, \tag{1}$$

where $\theta$ is the Bragg angle and $\beta$ is the full width at half maximum (FWHM) of the peak, while $\lambda$ is the X-ray wavelength. The obtained results are reported in Table 1. The results show that the average grain size increases from 20 to 67 nm with increasing of the deposition time. The increase of the crystallite size with the increase of deposition time can be explained as follows. As the deposition time increases, the amount of solute reaching the surface of the substrate increases to form film and therefore, the electrostatic interaction between solute atoms becomes larger, thereby increasing the probability of more solute to be gathered together to form a crystallite[24]. However, it is interesting to note that the average grain size increases slightly when the deposition time changes from 7 to 13 min. Such behavior of $In_2O_3$ grains was observed in several studies[25, 13].

Figure 3 shows the SEM surface and EDS analysis of the $In_2O_3$ thin films deposited at different deposition times. As the deposition time increases, changes in the morphology of the films are observed. It is interesting to note that, in the case of the films deposited at 4 min (Figure 3(a)) and 7 min (Figure 3(b)), grains with a pyramidal-shape are formed. While for the film deposited at 10 min (Figure 3(c)), in addition to the pyramid-shaped grains, we notice the emergence of other

Table 1. Grain size of $In_2O_3$ thin films as a function of deposition time (4–13 min).

| Deposition time (min) | Angle (deg) | $hkl$ | Crystallite size (nm) |
|---|---|---|---|
| 4 | 30.69 | 222 | 20 |
| 7 | 30.68 | 222 | 50 |
| | 35.58 | 400 | 48 |
| 10 | 30.70 | 222 | 58 |
| | 35.56 | 400 | 59 |
| 13 | 30.70 | 222 | 65 |
| | 35.57 | 400 | 67 |

grains that are granular in shape. The sample deposited at 13 min (Figure 3(d)) shows that the grains are granular in shape but seen to be densely packed. The difference in grain shapes probably suggests the difference in growth orientations and corroborates the XRD studies. The fact that the mean crystallite size obtained using Scherer's formula is in all cases substantially smaller than the dimension of the grain observed by the SEM images, indicating that these grains are probably aggregates of many crystallites of $In_2O_3$. The Gibbs free energy of the surface of nano crystals is usually high, and the grains have the tendency toward aggregate formation, thereby reducing the Gibbs free energy[26]. The forgoing discussion leads to the conclusion that the grains shape can be changed by varying the deposition time. These results are consistent with the fact the grain shape depends on the growth conditions[27]. Also the SEM surface images show that the film deposited at 13 min has less roughness than the other films. The less rough surface is probably due to the most preferential growth in the [100] direction over the entire surface. It was recently reported that the preferential growth induces flat surfaces of ITO films by Kim *et al.*[28]. Energy dispersive analyses of X-rays (EDAX) generated by the incident electron beam were carried out to investigate the composition of indium oxide films formed. All of the $In_2O_3$ films are composited from O and In atoms in addition to Si, which come from the substrate.

Figure 4 confirms that microstructure is greatly influenced by the deposition time. From Figure 4(a) it is observed that some grains grew in the through-thickness direction, but others did not. It can also be seen in Figure 4(b) that there is a very clear columnar structure. Furthermore, it is clear that the thicker film consists of two layers. Qiao *et al.* reported the similar results[14]. The good cohesion between the $In_2O_3$ thin film and the glass substrate is obviously observed.

The optical transmittance measured as a function of the wavelength is depicted in Figure 5. The deposition time exhibits a significant impact on the optical transmittance of films, a maximum visible transmittance (VT) of $\sim$ 93% is observed at $\sim$ 709 nm for the films prepared at 13 min (thickness of this film = 725 nm), whereas the smallest optical transmittance (VT) of $\sim$ 79% is observed at $\sim$ 628 nm for the film prepared at 4 min (thickness of this film = 395 nm) despite the fact that this film is thinner than the other films. A similar observation has been found by another researcher[30]. The higher transmittance observed in the films is attributed to a decline of scattering effects, structural homogeneity and better crystallinity, whereas low transmittance observed in the layer might be due to the less crystallinity leading to more light scat-

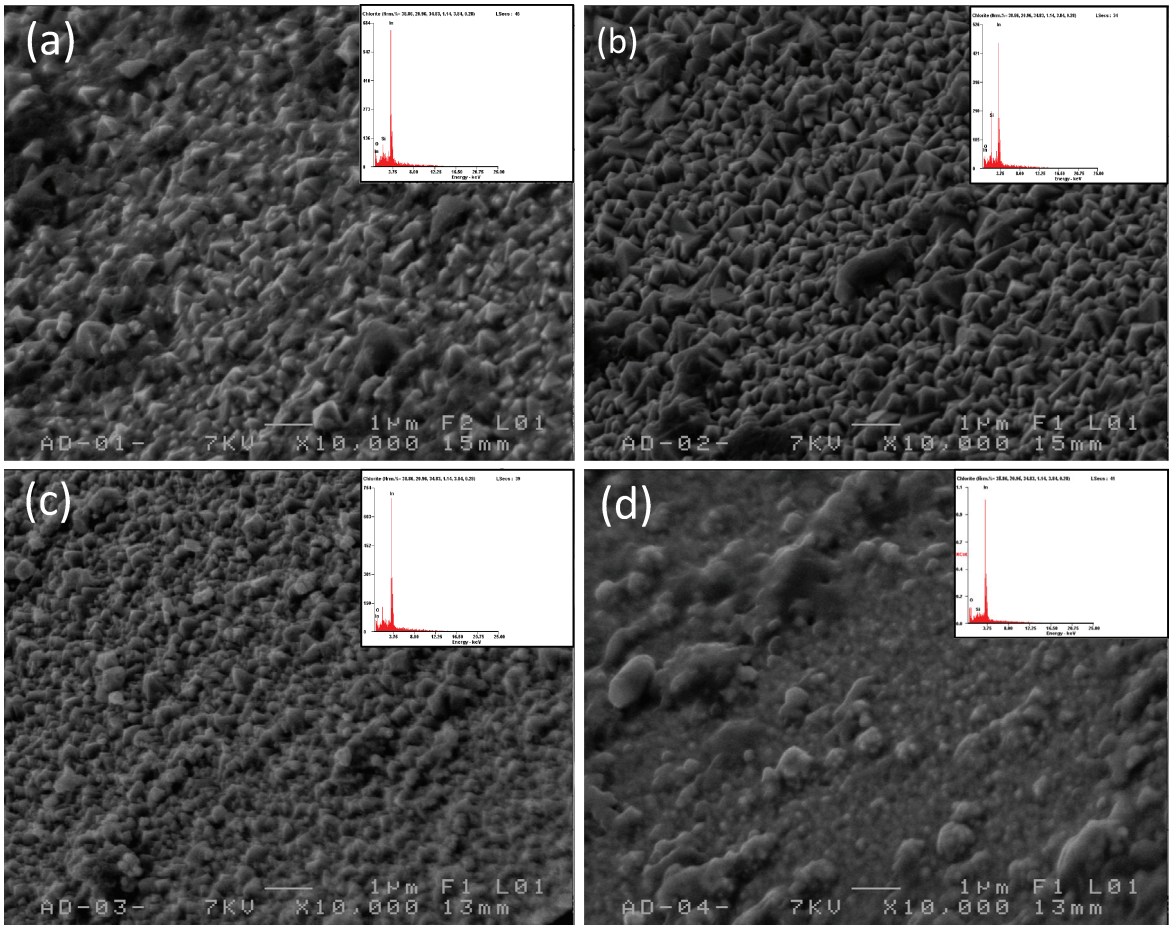


Figure 3. SEM surface and EDS analysis of the $In_2O_3$ thin films deposited at various deposition time of (a) 4 min, (b) 7 min, (c) 10 min, and (d) 13 min.

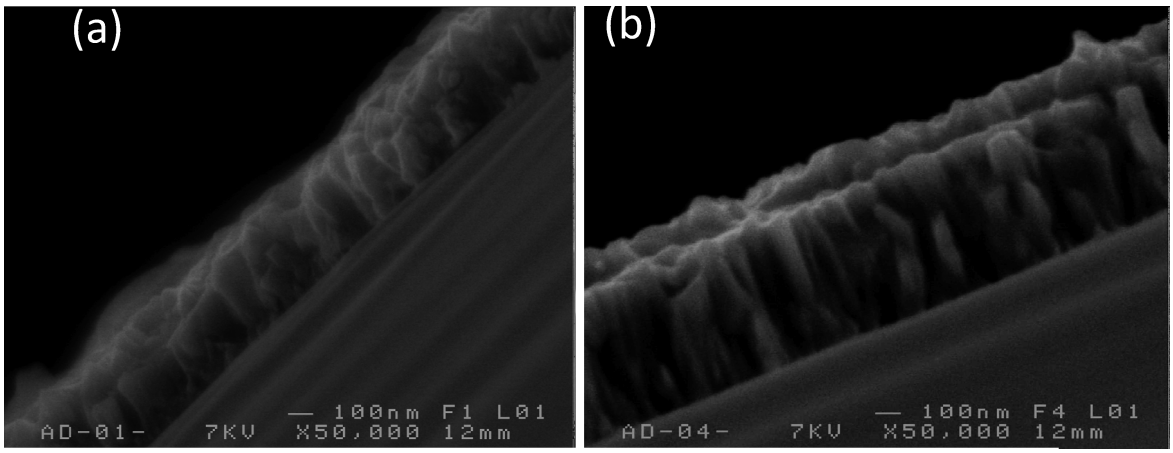


Figure 4. Cross-sectional images of the $In_2O_3$ thin films deposited at various deposition time of (a) 4 min and (b) 13 min.

tering[29]. On the other hand, the high transmittance of the film deposited at 13 min is due to the less roughness of this film. It is well known that a rough surface causes light scattering, resulting in transmittance reduction. In conclusion, the maximum visible transmittance value of films is the result of the combination of several effects: structural homogeneity, better crystallinity and the smooth surface.

The optical band gap of $In_2O_3$ films is estimated from Tauc relationship[31]:

$$(\alpha h\nu)^2 = A(h\nu - E_g), \tag{2}$$

where $\alpha$ is the absorption coefficient, $A$ is the constant independent of photon energy ($h\nu$), $h$ is the Planck constant, and $E_g$ is the optical band gap. The values of the optical band gap are obtained by extrapolating the tangential line of the data to the abscissa axis in the plot of $(\alpha h\nu)^2$ as a function of $h\nu$ as shown in Figure 6. Film deposited at 4 min has low band gap

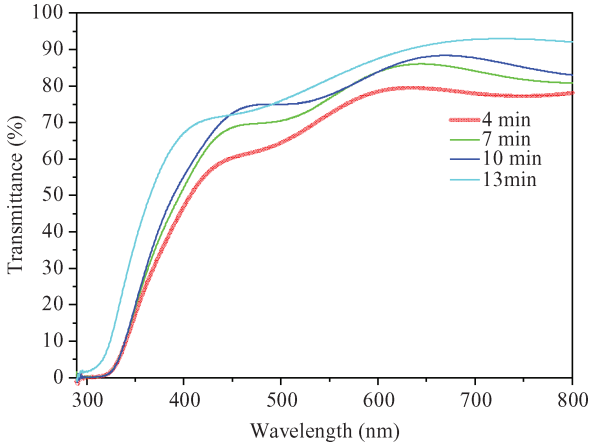


Figure 5. (Color online) Optical transmittance spectra of $In_2O_3$ thin films as a function of deposition time.

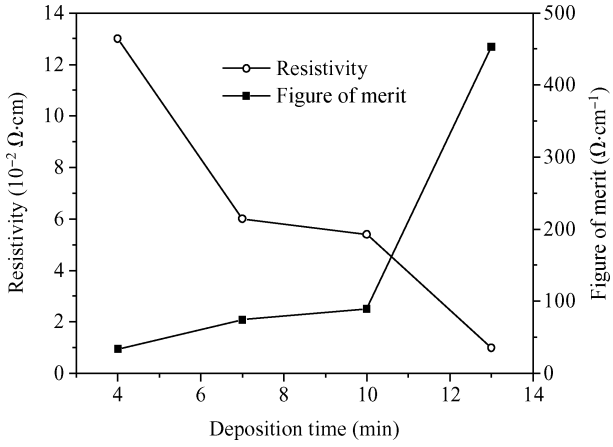


Figure 7. Electrical resistivity, and figure of merit of $In_2O_3$ thin film deposited at various deposition times.

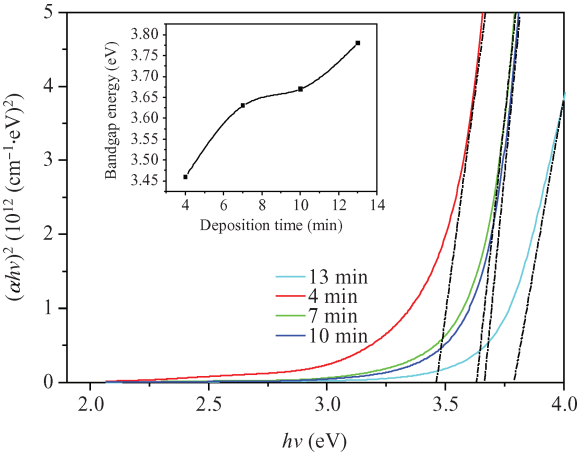


Figure 6. (Color online) Optical band gap energy for the $In_2O_3$ thin films deposited at various deposition time.

3.46 eV, this is due to the presence of an amorphous phase in this film network as deduced from the XRD. Amorphous phase is generally accompanied by a disorder in the film network. For highly disordered film, the band tail width (Urbach tail) is large; consequently the optical band gap is narrowed. This situation is reported in amorphous silicon thin films a-Si:H[32] and silicon nitride thin films a-Si:N[33]. They have also found the optical band gap shift towards the lower energies induced by a disorder in the film network[34, 35]. The optical gap of films which deposited at 7, 10, and 13 min is close to its value for $In_2O_3$ bulk material. This is due to the good crystallinity of these films.

Similar values of optical band gap have been found by other researchers[36, 37].

Figure 7 shows the dependence of electrical resistivity ($\rho$) and figure of merit on deposition time. Resistivity decreases continuously with an increase in the deposition time. They have also observed a decrease in the resistivity of $In_2O_3$ thin films with increasing of deposition time[16]. The electrical resistivity is improved, due to the grain coalescence structure and the lowest resistivity of $10^{-2}$ Ω·cm is obtained. This is mainly attributed to the decreasing of the number of scattering centers and trapping centers in the grain boundaries in which the high dense and packed grains cause an increase of carrier mobility and electron concentration[38, 39]. This is supported by the SEM surface images and XRD analysis which indicate that the increase of deposition time gives more tightly packed grains and large grains size, respectively. A similar variation of the resistivity with the improvement in the crystallinity is reported in Ti-doped indium oxide films[40].

The figure of merit is known to be an index for evaluating the performance of transparent conducting films, and it is given by the equation $F = (-\rho \ln T)^{-1}$, where $\rho$ is the electrical resistivity and $T$ is the average transmittance in the wavelength range of 400–800 nm[41]. The figure of merit for the $In_2O_3$ thin film deposited at 4 min was estimated as 33.61 $\Omega^{-1}$ cm$^{-1}$. As the deposition time increases to 13 min, the figure of merit increases to 453 $\Omega^{-1}$ cm$^{-1}$ (see Figure 7). The increase in the figure of merit results from the decrease in the electrical resistivity with increasing deposition time. The experimental data suggest that a deposition time of 13 min is the best condition for depositing high-quality $In_2O_3$ films.

## 4. Conclusion

The effect of the deposition time on the crystalline state, surface morphology, optical, and electrical properties of $In_2O_3$ films was investigated. X-ray diffraction reveals a polycrystalline nature for all films with a preferred grain orientation along the (222) plane when the deposition time changes from 4 to 10 min, but when the deposition time equals 13 min we found that the majority of grains preferred the (400) plane. SEM images show that the films are rough surface and the shape of grains changes with the change of the preferential growth orientation.

The optical characterization showed that our films are transparent. The transmittance improvement of $In_2O_3$ films was closely related to the good crystalline quality of the films. We have found also that the optical gap is varied between 3.46 eV and 3.79 eV, and the values of resistivity are found between 13 × $10^{-2}$ Ω·cm and $10^{-2}$ Ω·cm. Finally, we conclude that the deposition time is an interesting factor for controlling the quality of the thin films deposited by the ultrasonic spray technique.

## References


[1] Hartnagel H L, Dawar A L, Jain A K, et al. Semiconducting transparent thin films. Bristol and Philadelphia: IOP Publishing, 1995

[2] Girtan M, Cachet H, Rusua G I. On the physical properties of indium oxide thin films deposited by pyrosol in comparison with films deposited by pneumatic spray pyrolysis. Thin Solid Films, 2003, 427: 406

[3] Prince J J, Ramamurthy S, Subramanian B, et al. Spray pyrolysis growth and material properties of $In_2O_3$ films. J Cryst Growth, 2002, 240: 142

[4] Chen Z, Yang K, Wang J. Preparation of indium tin oxide films by vacuum evaporation. Thin Solid Films, 1988, 162: 305

[5] Qiao Z, Mergel D. Comparison of radio-frequency and direct-current magnetron sputtered thin $In_2O_3$:Sn films. Thin Solid Films, 2005, 484: 146

[6] Kulkarni A K, Schulz K H, Lim, et al. Dependence of the sheet resistance of indium-tin-oxide TS thin films on grain size and grain orientation determined from X-ray diffraction techniques. Thin Solid Films, 1999, 345: 273

[7] Ayeshamariam A, Kashif M, Bououdina M, et al. Morphological, structural, and gas-sensing characterization of tin-doped indium oxide nanoparticles. Ceramics International,2014, 40: 1321

[8] Marotta V, Orlando S, Parisi G P, et al. Electrical and optical characterization of multilayered thin film based on pulsed laser deposition of metal oxides. Appl Surf Sci, 2000, 168: 141

[9] Parthiban S, Ramamurthi K, Elangovan E, et al. High-mobility molybdenum doped indium oxide thin films prepared by spray pyrolysis technique. Mater Lett, 2008, 62: 3217

[10] Parthiban S, Elangovan E, Ramamurthi K, et al. Investigations on high visible to near infrared transparent and high mobility Mo doped $In_2O_3$ thin films prepared by spray pyrolysis technique. Solar Energy Materials & Solar Cells, 2010, 94: 406

[11] Powder diffraction file, Joint Committee on Powder Diffraction Standards, ASTM, Philadelphia, PA, JCPDS ICDD, 1991, card 6-416

[12] Korotcenkov G, Cerneavschi A, Brinzari V, et al. $In_2O_3$ films deposited by spray pyrolysis as a material for ozone gas sensors. Sensors and Actuators B, 2004, 99: 298

[13] Korotcenkov G, Brinzari V, Cerneavschi A, et al. Crystallographic characterization of $In_2O_3$ films deposited by spray pyrolysis. Sens Actuators B, 2002, 84(1): 37

[14] Shigesato Y, Paine D C. A microstructural study of low resistivity tin-doped indium oxide prepared by D.C. magnetron sputtering. Thin Solid Films, 1994, 238: 44

[15] Zhang K H L, Walsh A, Catlow C R A, et al. Surface energies control the self-organization of oriented $In_2O_3$ nanostructures on cubic zirconia. Nano Lett, 2010, 10: 3740

[16] Lee J H, Park B O. Transparent conducting InO thin films prepared by ultrasonic spray 23pyrolysis. Surface and Coatings Technology, 2004, 184: 104

[17] Vaishnav V S, Patel P D, Patel N G. Preparation and characterization of indium tin oxide thin films for their application as gas sensors. Thin Solid Films, 2005, 487: 277

[18] Terzini E. Properties of ITO thin films deposited by RF magnetron sputtering at elevated substrate temperature. Mater Sci Eng B, 2000, 77: 110

[19] Pham D P, Phan B T, Hoang V D. Control of preferred (222) crystalline orientation of sputtered indium tin oxide thin films. Thin Solid Films, 2014, 570: 16

[20] Sun S W, Wang L D, Kwok H S. Improved ITO thin films with a thin ZnO buffer layer by sputtering. Thin Solid Films, 2000, 360: 75

[21] Qiao Z, Latz R, Mergel D. Thickness dependence of $In_2O_3$:Sn film growth. Thin Solid Films, 2004, 466: 256

[22] Saxena A K, Singh S P, Thangaraj R, et al. Thickness dependence of the electrical and structural properties of $In_2O_3$:Sn films. Thin Solid Films, 1984, 117: 95

[23] Klug H P, Alexander L E. X-ray diffraction procedures. 3rd ed. New York: Wiley, 1974: 966

[24] Rao T P, Kumar M C S. Effect of thickness on structural, optical and electrical properties of nanostructured ZnO thin films by spray pyrolysis. Appl Surf Sci, 2009, 255: 4579

[25] Amaral A, Brogueira P, de Carvalho C N. Early stage growth structure of indium tin oxide thin films deposited by reactive thermal evaporation. Surface and Coatings Technology, 2000, 125: 154

[26] Zhu J, Chan H, Liu H, et al. Needle-shaped nanocrystalline CuO prepared by liquid hydrolysis of $Cu(OAc)_2$. Mater Sci Eng A, 2004, 384: 172

[27] Son C S, Kim S M, Kim Y H, et al. Deposition-temperature dependence of ZnO/Si grown by pulsed laser deposition. J Korean Phys Soc, 2004, 45: S685

[28] Kim H, Horwitz J S, Kim W H, et al. Highly oriented indium tin oxide films for high efficiency organic light-emitting diodes. J Appl Phys, 2002, 91: 5371

[29] Khatibani A B, Ziabari A A, Rozati S M, et al. Characterization and gas-sensing performance of spraypyrolysed $In_2O_3$ thin films: substrate temperature effect. Trans Elect Electron Mater, 2012, 13: 111

[30] Bu I Y Y. A simple annealing process to obtain highly transparent and conductive indium doped tin oxide for dye-sensitized solar cells. Ceramics International, 2014, 40: 3445

[31] Khan M A M, Khan W, Ahamed M. Structural and optical properties of $In_2O_3$ nanostructured thin film. Mater Lett, 2012, 79: 120

[32] Street R A. Hydrogenated amorphous silicon. Cambridge University Press, 1991: 92

[33] Aida M S, Attaf A, Benkedir M L. The optical properties of sputtered amorphous silicon nitride films: effect of RF power. Phil Mag B, 1996, 73: 339

[34] Moualkia H, Hariech S, Aida M S, et al. Growth and physical properties of CdS thin films prepared by chemical bath deposition. J Phys D: Appl Phys, 2009, 42: 135404

[35] Ilican S, Caglar Y, Caglar M, et al. Polycrystalline indium-doped ZnO thin films: preparation and characterization. J Optoelectron Adv Mater, 2008, 10: 2592

[36] Girtan M, Folcher G. Structural and optical properties of indium oxide thin films prepared by an ultrasonic spray CVD process. Surface and Coatings Technology, 2003, 172: 242

[37] Jothibas M, Manoharan C, Ramalingam S. Preparation, characterization, spectroscopic (FT-IR, FT-Raman, UV and visible) studies, optical properties and Kubo gap analysis of $In_2O_3$ thin films. Journal of Molecular Structure, 2013, 1049: 239

[38] Song D, Widenborg P, Chin W. Investigation of lateral parameter variations of Al-doped zinc oxide films prepared on glass substrates by RF magnetron sputtering. Solar Energy Materials & Solar Cells, 2002, 73: 17

[39] Kim H, Horwitz J S, Kushto G P, et al. Transparent conducting Zr-doped $In_2O_3$ thin films for organic light-emitting diodes. Appl Phys Lett, 2001, 78: 1050

[40] Gupta R K, Ghosh K, Mishra S R. High mobility Ti-doped $In_2O_3$ transparent conductive thin films. Mater Lett, 2008, 62: 1033

[41] Senthilkumar V, Vickraman P. Annealing temperature dependent on structural, optical and electrical properties of indium oxide thin films deposited by electron beam evaporation method. Curr Appl Phys, 2010, 10: 880